Journal of Power Sources 268 (2014) 712–717

Contents lists available at ScienceDirect

Journal of Power Sources

journal homepage: www.elsevier.com/locate/jpowsour

Short communication

Pt-coated Pd nanocubes as catalysts for alkaline oxygen reduction activity

Chien-Liang Lee*, Chia-Chen Yang, Chia-Ru Liu, Zhe-Ting Liu, Jyun-Sian Ye

Department of Chemical and Materials Engineering, National Kaohsiung University of Applied Sciences, Kaohsiung 807, Taiwan

HIGHLIGHTS

- A simple method for synthesizing Pt-coated Pd nanocubes has been developed.
- The Pt shell is grown on a cubic Pd seed via an epitaxial model.
- These bimetallic nanocubes are used for catalyzing alkaline ORR.
- The core–shell nanocubes show 2.6 times higher specific activity than Pt nanoparticles.

GRAPHICAL ABSTRACT

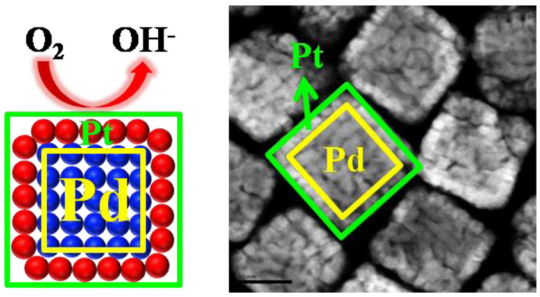

ARTICLE INFO

Article history:
Received 3 January 2014
Received in revised form
13 June 2014
Accepted 19 June 2014
Available online 7 July 2014

Keywords:
ORR
(100)
Crystal faces
Core–shell

ABSTRACT

Pt-coated Pd nanocubes enclosed with (100) planes were successfully synthesized using an epitaxial approach. Their microstructures were determined on the basis of their electron diffraction patterns and line scan energy-dispersive X-ray measurements by spotting on a single nanocube. These bimetallic nanocubes can be used as catalysts for an alkaline oxygen reduction reaction. The results of the rotating ring-disk electrode measurements indicated that these nanocubes displayed a 2.6 times greater specific activity than Pt nanoparticles.

1. Introduction

One of the major goals in the development of alkaline fuel cells is the establishment of highly active catalysts, particularly for the oxygen reduction reaction (ORR). Pt catalysts are currently used commercially to catalyze the ORR [1]. However, recent studies [2,3] have indicated that platinum has reduced catalytic activity in alkaline solutions, resulting in excessive production of HO_2^- on the Pt surface, which limits the efficiency of the ORR. To improve its activity, a new catalyst that consists of a monolayer of Pt coated on another metal substrate has been designed [4,5]. In this core–shell–like model, the activity of the Pt shell is strongly dependent on the substrate metal [4,5]; thus, a volcano relationship is obtained from the plot of the activity of the Pt shell on various substrates as a function of the calculated metal d-band center [4]. Unlike Ru, Ir, Rh, and Au, the use of Pd as a substrate ensures relatively good activity in alkaline electrolytes [4]. Furthermore, based on this related finding, Pt-coated Pd nanoparticles showed higher activity than Pt catalysts during the ORR in alkaline electrolytes [6].

Another efficient approach for improving the electrochemical properties of catalysts is to control the microstructure of the

* Corresponding author. Tel.: +886 7 3814526x5131; fax: +886 7 3830674.
E-mail addresses: cl_lee@kuas.edu.tw, cl_lee@url.com.tw (C.-L. Lee).

http://dx.doi.org/10.1016/j.jpowsour.2014.06.112
0378-7753/

catalyst. Several elegant studies [7–9] have identified that the ORR is sensitive to the enclosed planes of the catalyst. Adzić and colleagues [10] reported that the half-wave potential of Au(100) was more positive than that of Au(111) and Au(110) for alkaline ORRs. A series pathway for a four-electron mechanism on the Au(100) was demonstrated. The stronger interaction between O_2, O_2^-, and HO_2^- and Au(100) was proposed to be the origin of the high activity. Prieto et al. further confirmed the higher activity of Au(100) compared to Au(111) and Au(110) [11]. Tammeveski and colleagues [12] further demonstrated that the ORR activity of Pd nanoparticles in alkaline media was lower than that of Pd nanocubes. Accordingly, they concluded that the specific activity of 26.9 nm Pd nanocubes enclosed with (100) planes was 3.8 times that of 2.8 nm Pd nanoparticles, for which the Pd(111) planes formed the predominate facets. In addition, we previously reported a systematic comparison of the catalytic activity of differently sized Pd nanocubes and small Pd nanoparticles for the alkaline ORR [13]. The 27 nm Pd nanocubes exhibited a higher kinetic current and specific activity compared to the 9-nm Pd nanoparticles. Thus, the crystal face at the surface of the catalysts, composed of metallic nanomaterials with various shapes, had a major effect on the electrocatalytic reaction. In this study, Pt-coated Pd nanocubes enclosed with (100) planes were successfully prepared and used to catalyze ORRs in 1 M NaOH solutions. The specific activities of Pt-coated Pd nanocubes and Pt nanoparticles were also compared.

2. Experimental methods

To synthesize Pt-coated Pd nanocubes via epitaxial growth, cubic Pd nanocores were initially prepared according to a previous report [14] as follows: 500 μL of 0.01 M H_2PdCl_4 aqueous solution was added to 10 mL of 1.25×10^{-2} M hexadecyltrimethyl ammonium bromide (C_{16}TAB) aqueous solution at a fixed temperature of 95 °C. After mixing, 80 μL of 0.1 M ascorbic acid was gradually added to the solution to generate a dark brown solution containing 27 nm Pd nanocubes. This Pd nanocube solution was used as the seed solution for growing Pt-coated Pd nanocubes by adding 40 μL of 0.1 M ascorbic acid and 500 μL of 0.01 M H_2PtCl_6, followed by stirring for 2 h at 95 °C to generate core–shell Pd–Pt nanocubes with 3.7 nm shells. Synthesis of Pt nanoparticles was similar to the synthesis of Pd nanocubes except that 1 mL of H_2PtCl_6 (0.01 M) aqueous solution was used instead of 500 μL of 0.01 M H_2PdCl_4 aqueous solution and the reducing agent was 1 M $NaBH_4$ solution (0.36 mL).

Characteristics, such as size, microstructure, and composition, of the prepared nanocubes were determined using high-resolution transmission electron microscopy (HR-TEM; JEOL JEM-2100F), energy-dispersive X-ray spectroscopy (EDX), and X-ray diffraction spectroscopy (XRD; Bruker D8; Cu anode; 1.54184 Å).

The electrochemical activities of the prepared Pt-coated Pd nanocubes, Pd nanocubes, and Pt nanoparticles as catalysts for use in cyclic voltammetry (CV) or linear scan voltammetry (LSV) experiments were evaluated using rotating ring-disk electrode (RRDE) measurements. First, a solution containing 35.7 μg cm^{-2} of the prepared catalyst and 17.8 μL of 0.25 wt% polyvinyl alcohol was dropped onto a 0.196 cm^2 glassy carbon electrode disk, which was then heated to 60 °C to evaporate the water. The RRDE measurements were performed using a combination of an RRDE system (AFMSRCE, Pine Research Instrumentation) and a bipotentiostat (CHI 727D). A catalyst-modified rotating glassy carbon disk platinum ring electrode (ring area: 0.11 cm^2) was used as the working electrode. In addition, a Pt counter electrode and Ag/AgCl (3 M KCl) reference electrode were used to measure the N_2- or O_2-saturated 1 M $NaOH_{(aq)}$ solutions. For the LSV measurements, the ring potential was maintained at 0.144 V (vs. Ag/AgCl) to oxidize the HO_2^- generated by O_2 reduction at the disk electrode. The collection efficiency (N) of the ring electrode, which was obtained by reducing ferricyanide at the disk electrode, was determined to be approximately 0.192. All potentials in the voltammogram were in reference to the reversible hydrogen electrode (RHE).

3. Results and discussion

Fig. 1A and B shows transmission electron microscopy (TEM) images of the nanoparticles prepared with and without, respectively, the sequential addition of H_2PtCl_6. Fig. 1A clearly shows many uniform cubic nanoparticles with larger nanocubes than those in Fig. 1B. The edge lengths of these nanocubes were calculated from the TEM results and are summarized in Fig. 1C. Previously, we determined that the mean edge length of the Pd nanocubes generated using the same method was 27 nm (Fig. 1B) [15]. For larger nanocubes grown via sequential addition of Pt salts, the mean edge length of the nanocubes shown in Fig. 1A is ~34.4 nm.

To identify the crystalline structure and composition of the nanocubes, dark-field TEM images, EDX spectra, electron diffraction (ED), and XRD patterns were examined. Typically, heavier atoms show a brighter contrast in dark-field images. As shown in Fig. 1D, the dark-field TEM image clearly revealed nanocubes constructed of uniformly brighter shells and darker cores. The atoms in the outer shell were significantly different from those in the inner core.

In addition, EDX line scan analysis was performed on a captured image of the nanocubes, as shown in Fig. 1E. We detected a stronger Pt signal for the nanocube shell compared to the center, whereas a strong Pd signal was detected from the nanocube center. These results indicated that the nanocube shell consisted of Pt, as labeled in Fig. 1D. The EDX analysis on composition afforded Pt and Pd atomic percentages for 35.13% and 64.87%, respectively. Fig. 1F demonstrated the ED pattern of a single core–shell nanocube. The bright spots in the ED pattern indicated that the nanocubes were single crystalline and enclosed by {100} planes. It was previously confirmed that (100) planes enclosed the Pd nanocubes [15]. In addition, the cell parameter of Pt was 3.924 Å and closed at 3.890 Å, which is the cell parameter of Pd [16]. The atomic radius of Pt is 1.376 Å, which is similar to the atomic radius of Pd (1.387 Å). The ED pattern suggested that the added Pt ions can be reduced and then deposited onto the surface of cubic Pd seeds via epitaxial growth. Fig. 1G shows the XRD pattern for the core–shell nanocubes. The strong peak at 46.6° and the small peak at 40° are similar to the peaks of the (100) and (111) diffraction planes in a standard Pd spectrum (JCPDS 88-2335), respectively. The strong (100) peaks showed the predominance of (100) facets for the nanocubes. The negligible peak corresponding to the Pt layers suggests the formation of very thin layers, which can be confirmed by the XRD patterns of core–shell Pd–Pt nanoparticles [17].

The catalytic activity of these nanocubes towards ORR was then examined, and their electrochemical properties were initially measured using CV. Fig. 2A shows a comparison of the CV curves obtained from measuring the electrochemical responses of the Pt-coated Pd nanocubes compared to those of the Pd nanocubes and Pt nanoparticles in 1 M $NaOH_{(aq)}$ solutions under a N_2 atmosphere. For the 27-nm Pd nanocubes, the area of repose between 0.14 and 0.44 V was associated with hydrogen adsorption/desorption onto the Pd surface. The poorly defined hydrogen adsorption region is due to the occurrence of both adsorbed and absorbed hydrogen [3]. The current for the electro double layer is evident from 0.44 to 0.64 V. Pd oxidation on the Pd nanocubes was initiated at 0.74 V, and we detected the reduction peak of PdO at 0.79 V. For 14.4 nm Pt nanoparticles (inset) with predominantly (111) facets, as confirmed by the inset of Fig. 1G, the two significant pairs of peaks between

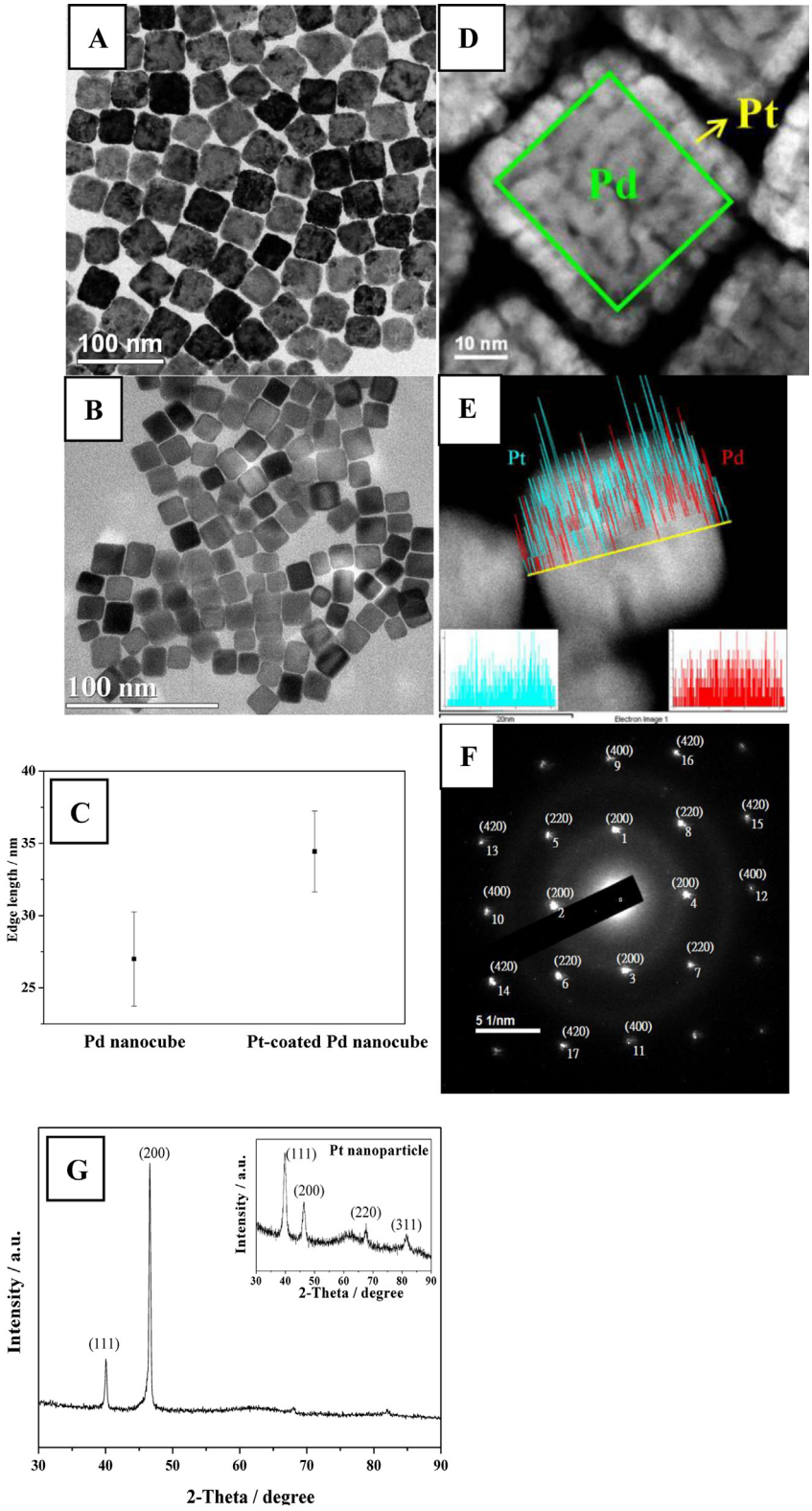

Fig. 1. Pt-coated Pd nanocubes (A, D, E–G) and cubic Pd seeds (B): (A–B) TEM images, (C) statistics for the edge lengths, (D) dark-field TEM image, (E) EDX line scan analysis, (F) electron diffraction pattern, and (G) X-ray diffraction pattern (inset: Pt nanoparticle).

0.44 and 0.14 V were assigned to hydrogen adsorption and desorption. Upon positive scanning above 0.59 V, Pt–OH begins to form, and the maximum current was 0.84 V; beyond this value, PtO is produced. A strong peak for PtO reduction was obtained at 0.81 V during negative scanning. For the Pt-coated Pd nanocubes, we observed one paired peak between 0.29 and 0.32 V, which corresponded to hydrogen adsorption and desorption. Compared to the results of the Pd nanoparticles, the hydrogen region was relatively

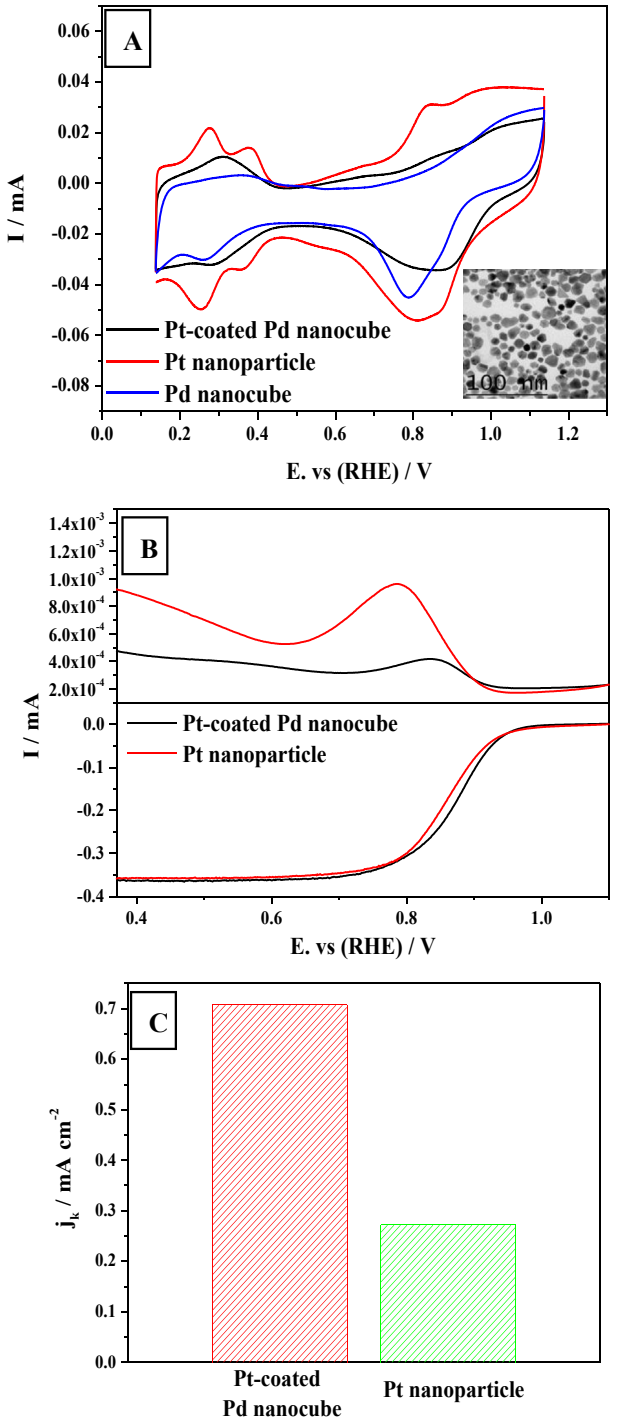

Fig. 2. Electrochemical properties: (A) CV curves of the Pt-coated Pd nanocubes, cubic Pd seeds, and Pt nanoparticles in 1 M NaOH electrolyte (scan rate: 50 mV s^{-1}). Inset: TEM image of the Pt nanoparticles, (B) LSV curves of the Pt-coated Pd nanocubes and Pt nanoparticles obtained by RRDE experiments in O_2-saturated NaOH electrolyte (scan rate: 10 mV s^{-1}; rotating speed of electrode: 1600 rpm), and (C) comparative bar plots of the specific activities (j_ks) of the Pt-coated Pd nanocubes and Pt nanoparticles.

strong. The reduction peak for the Pt oxides was observed at 0.89 V; the overpotential was lower than those for the reductions of PdO on Pd nanocubes and PtO on Pt nanoparticles.

Importantly, the 34.4-nm Pt-coated Pd nanocubes showed higher ORR activity than the 14.4 nm Pt nanoparticles. Fig. 2B demonstrated the LSV curves for O_2 reduction catalyzed by the Pt-coated Pd nanocubes and Pt nanoparticles dispersed on disk electrodes, wherein HO_2^- production was measured in situ using the Pt ring electrode in the 1 M $NaOH_{(aq)}$ electrolyte. For the disk current (I_d) generated by the nanocubes, the activation-controlled region was evidently higher than 0.94 V, and the activation–diffusion mixed-controlled region occurred between 0.94 and 0.79 V. Beyond 0.79 V was the diffusion-controlled section, which was characterized by a minimum O_2 concentration at the nanocube surface. Relative to the Pt nanoparticles, the significant difference between the nanocubes and nanoparticles was their potential before the mixed-controlled region for the ORR. The nanocubes have a greater ORR current than the nanoparticles before 0.8 V. This finding indicated that the reaction proceeds rapidly on the active site of the nanocubes. Importantly, the Pt-coated Pd nanocubes have a lower ring current (I_r) than the Pt nanoparticles: larger I_r values indicate the production of more HO_2^-, which results from slow kinetics.

Pt is a well-known and commercial, but expensive, catalyst for alkaline ORRs [2,18,19]. To accurately compare the specific activities demonstrated by the Pt-coated Pd nanocubes and Pt nanoparticles towards the ORR in 1 M $NaOH_{(aq)}$ electrolyte, the mass-transfer–corrected kinetic currents were normalized to the electrochemical surface area (ESA) using the RRDE results obtained from Fig. 2B. On the basis of a detailed study of comparable Pt catalysts for the ORR involving a thin-film rotating disk experiment [20], the specific activity in terms of kinetic current (j_k) can be calculated using

$$j_k = \frac{\frac{i_d \times i}{i_d - i}}{\mathrm{ESA}} = \frac{i_k}{\mathrm{ESA}}, \quad (1)$$

where i_d is the diffusion-limiting current at 0.6 V, i_k is the kinetic current, and the ESA for core–shell nanocubes and Pt nanoparticles are 0.205 and 0.371 cm^2, respectively, which are estimated by the hydrogen desorption charge over 210 μC cm^{-2} in the CV curves of Fig. 2A. Here, 210 μC cm^{-2} is the charge required to oxidize a monolayer of H_2 on Pt [21,22]. The i_k values at 0.9 V for the nanocube and nanoparticle catalysts are 1.45×10^{-1} and 1.01×10^{-1} mA, respectively. Note that the core–shell nanocubes showed a specific activity that was 2.6 times higher than the nanoparticles in the comparative bar plots (Fig. 2C), where the j_ks for nanocubes and nanoparticles were 0.708 and 0.272 mA cm^{-2}, respectively. The activity of the Pt outer shell can be improved when the Pd nanocubes are used as support. The higher activity could be ascribed to an electronic interaction between the Pt shell and Pd substrate, resulting in an optimum balance between the O–O bond breaking and O–H bond-making activity [4].

In addition, at 0.9 V, the fraction of OH_2^- produced can be calculated using the following equation [23]:

$$X_{OH_2^-} = \frac{2\frac{I_r}{N}}{I_d + \frac{I_r}{N}}, \quad (2)$$

The $X_{OH_2^-}$ values of the bimetallic nanocube and Pt catalysts are 2.65 and 3.44%, respectively. At the same potential, the electron transfer number (n) involved in the ORRs can be calculated via [24]

$$n = 4 - 2\left(\frac{I_r}{I_d \times N}\right), \quad (3)$$

The n values are 3.97 and 3.96 for the Pt-coated Pd nanocubes and Pt catalysts, respectively. This indicates that, within the activation-controlled region, the ORR proceeds slightly faster on the Pt(100) on the Pd nanocube.

Furthermore, the ORR electrocatalytic stability and durability for the Pt-coated Pd nanocubes compared to the Pt nanoparticles were

studied using a repeated LSV test. Fig. 3A shows a TEM image of Pt-coated Pd nanocubes after the 1000 cycle test. The nanocubes became more spherical and slightly aggregated. Consistent with the line-scanning EDX data (the inset of Fig. 3A), the core–shell structure for the nanocube after the stability test remained. Fig. 3B shows a TEM image of the Pt nanoparticles after the same cycle test. Interestingly, the Pt nanoparticles were dramatically aggregated and melted to become a network structure. Fig. 3C shows a comparative plot for the decay percentages in i_k of the bimetallic nanocubes compared to the Pt nanoparticles at the first and 1000th cycle. Approximately 64.6% and 41.9% i_k for the nanocubes and nanoparticles were retained, respectively. Compared to the Pt nanoparticles, the greater i_k for the nanocubes was attributed to the high ESA stability (85.1%) of the nanocubes, which was measured and compared by the CV curves (Fig. 3D) at the first and 1000th cycle. The shape for these two CV curves was nearly unchanged. These results suggested that Pt-coated Pd nanocubes without the need for carbon supports can maintain ORR activity. Fig. 3E further showed the comparative CV curve for the Pt nanoparticles before and after 1000 repeated LSV scans. A significant reduction for hydrogen adsorption and desorption area below 0.43 V was observed after the cycle test. The low hydrogen region, resulting in a failed ESA calculation, was attributed to the aggregation of Pt nanoparticles, as shown in Fig. 3B.

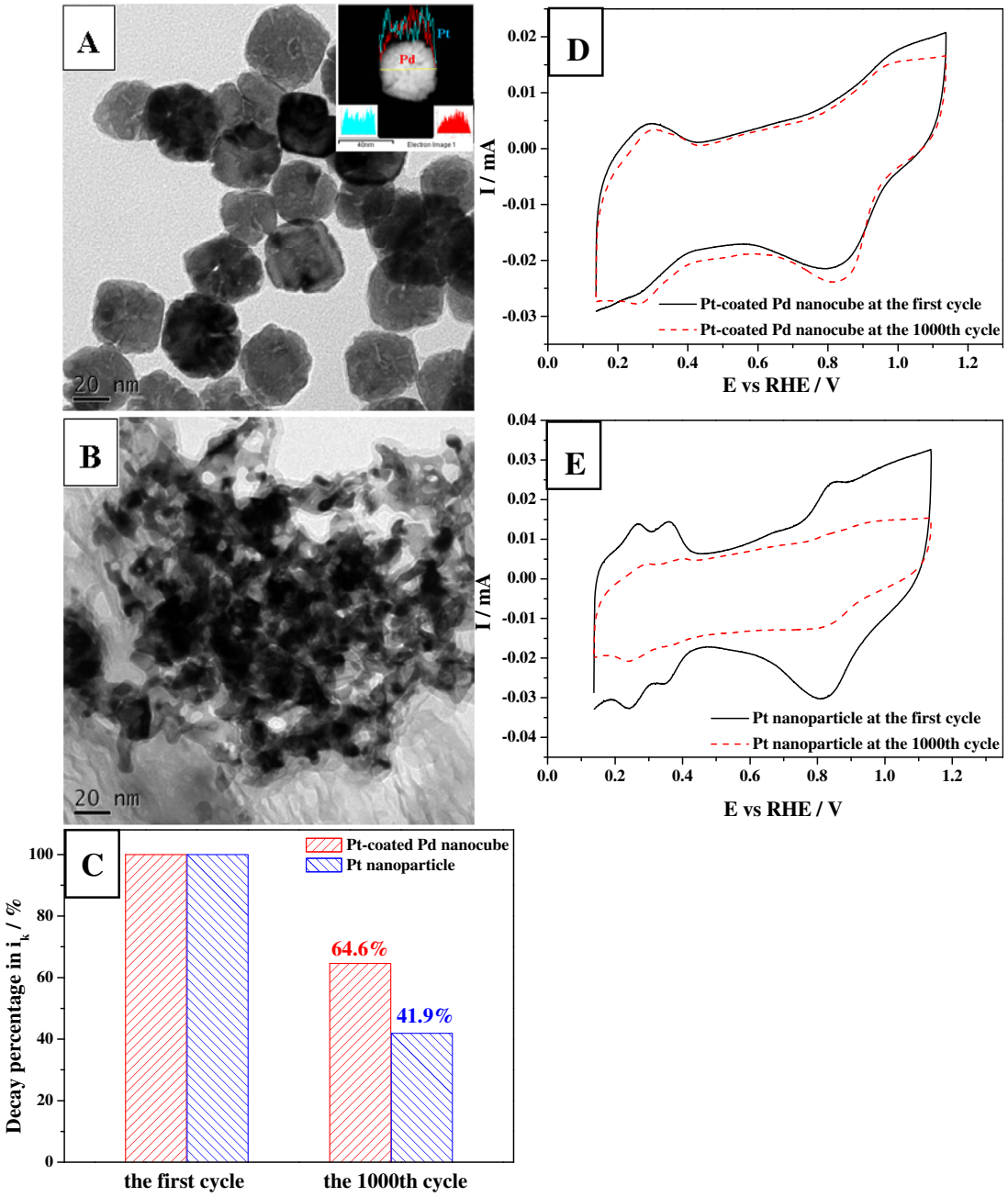

Fig. 3. Comparative stability tests of Pt-coated Pd nanocubes and Pt nanoparticles (A) TEM image of Pt-coated Pd nanocubes after 1000 LSV cycles (inset: line-scanned EDX), (B) TEM image of Pt nanoparticles after 1000 LSV cycles, (C) A comparison of the decay percentages in the i_ks for the Pt-coated Pd nanocubes and Pt nanoparticles between the first and 1000th LSV cycles in O_2-saturated NaOH electrolyte. (Scan rate: 50 mV s^{-1}. Rotating speed of the electrode: 400 rpm), (D) CV curves of Pt-coated Pd nanocubes before and after the 1000th LSV cycle (Scan rate: 50 mV s^{-1}), and (E) CV curves of Pt nanoparticles before and after the 1000th LSV cycle (Scan rate: 50 mV s^{-1}).

4. Conclusion

Pt-coated Pd nanocubes were successfully synthesized for oxygen electroreduction. On the basis of the results of the ED analysis, it was concluded that the bimetallic nanocubes essentially consisted of (100) planes. The Pt-coated Pd nanocubes had better electrocatalytic activity for the ORR than the Pt catalysts. The data provided by the RRDE measurements showed that the nanocubes exhibited higher specific activity than the Pt nanoparticles.

Acknowledgments

The authors would like to thank the Ministry of Science and Technology, Taiwan, for financially supporting this research under Contract No. 101-2628-E-151-001-MY2 and Mr. Shyne-Yen Yao at National Chen-Kung University and Mr. Hsien-Tsan Lin of Regional Instruments Center at National Sun Yat-Sen University for their helps in the TEM experiments.

References

[1] L.H. Jiang, A. Hsu, D. Chu, R.R. Chen, J. Electroanal. Chem. 629 (2009) 87.
[2] L. Genies, R. Faure, R. Durand, Electrochim. Acta 44 (1998) 1317.
[3] L. Jiang, A. Hsu, D. Chu, R. Chen, J. Electrochem. Soc. 156 (2009) B643.
[4] F.H.B. Lima, J. Zhang, M.H. Shao, K. Sasaki, M.B. Vukmirovic, E.A. Ticianelli, R.R. Adzic, J. Phys. Chem. C 111 (2007) 404.
[5] M. Shao, J. Power Sources 196 (2011) 2433.
[6] F.H.B. Lima, J. Zhang, M.H. Shao, K. Sasaki, M.B. Vukmirovic, E.A. Ticianelli, R.R. Adzic, J. Solid State Electrochem. 12 (2008) 399.
[7] B.B. Blizanac, P.N. Ross, N.M. Markovic, J. Phys. Chem. B 110 (2006) 4735.
[8] N.M. Markovic, H.A. Gasteiger, N. Philip, J. Phys. Chem. 100 (1996) 6715.
[9] M.I. Awad, T. Ohsaka, J. Power Sources 226 (2013) 306.
[10] R.R. Adzic, N.M. Markovic, V.B. Vesovic, J. Electroanal. Chem. 165 (1984) 105.
[11] A. Prieto, J. Hernandez, E. Herrero, J.M. Feliu, J. Solid State Electrochem. 7 (2003) 599.
[12] H. Erikson, A. Sarapuu, N. Alexeyeva, K. Tammeveski, J. Solla-Gullon, J.M. Feliu, Electrochim. Acta 59 (2012) 329.
[13] C.L. Lee, H.P. Chiou, C.R. Liu, Int. J. Hydrogen Energy 37 (2012) 3993.
[14] W.X. Niu, Z.Y. Li, L.H. Shi, X.Q. Liu, H.J. Li, S. Han, J. Chen, G.B. Xu, Cryst. Growth Des. 8 (2008) 4440.
[15] C.L. Lee, H.P. Chiou, Appl. Catal. B Environ 117 (2012) 204.
[16] D.R. Lide, CRC Handbook of Chemistry and Physics, 85th ed., Chemical Rubber Publishing Company, Boca Raton, 2004.
[17] L. Liu, G. Samjeske, S. Nagamatsu, O. Sekizawa, K. Nagasawa, S. Takao, Y. Imaizumi, T. Yamamoto, T. Uruga, Y. Iwasawa, J. Phys. Chem. C 116 (2012) 23453.
[18] T.J. Schmidt, V. Stamenkovic, P.N. Ross, N.M. Markovic, Phys. Chem. Chem. Phys. 5 (2003) 400.
[19] J.S. Spendelow, A. Wieckowski, Phys. Chem. Chem. Phys. 9 (2007) 2654.
[20] K.J.J. Mayrhofer, D. Strmcnik, B.B. Blizanac, V. Stamenkovic, M. Arenz, N.M. Markovic, Electrochim. Acta 53 (2008) 3181.
[21] N.R. Elezovic, B.M. Babic, L. Gajic-Krstajic, P. Ercius, V.R. Radmilovic, N.V. Krstajic, L.M. Vracar, Electrochim. Acta 69 (2012) 239.
[22] M.M. Dimos, G.J. Blanchard, J. Phys. Chem. C 114 (2010) 6019.
[23] A. Racz, P. Bele, C. Cremers, U. Stimming, J. Appl. Electrochem. 37 (2007) 1455.
[24] S.Q. Liu, J.Q. Xu, H.R. Sun, D.M. Li, Inorg. Chim. Acta 306 (2000) 87.